Proceedings of the 21st International Conference on Global Research and Education (Inter-Academia 2024)

A Numerical Tool for Spectral Analysis of Fiber Bragg Gratings written in Few-Mode Excited Optical Fibers

P. Pogorzelski[a], A. Anuszkiewicz[a,b], R. Buczyński[b,c] and T. Osuch[a,d,*]

[a] *Faculty of Electronics and Information Technology, Institute of Electronic Systems, Warsaw University of Technology, Nowowiejska 15/19, 00-665 Warsaw, Poland*
[b] *Institute of Microelectronics and Photonics, Łukasiewicz Research Network, Lotników 32/46, 02-668 Warsaw, Poland*
[c] *Faculty of Physics, University of Warsaw, Pasteura 5, 02-093 Warsaw, Poland*
[d] *National Institute of Telecommunications — National Research Institute, Szachowa 1, 04-894 Warsaw, Poland*

Doi: 10.12693/APhysPolA.146.490 *e-mail: tomasz.osuch@pw.edu.pl

This paper focuses on the spectral analysis of fiber Bragg gratings written in nanostructured large mode area and few-mode fibers when fundamental and higher mode(s) are simultaneously excited. For this purpose, an advanced numerical tool was developed and validated. A method for modal decomposition and superposition was proposed, which overcomes the limitations of commercial software. In the presented approach, the intermodal coupling as a consequence of non-ideal fringe pattern spatial distribution in fiber Bragg gratins is also considered. The numerical tool increases the versatility of fiber Bragg grating spectral analysis, especially taking into account the unconventional optical fibers having independent photosensitivity and refractive index profiles and few-mode operation.

topics: fiber Bragg grating (FBG), large mode area fibers, intermodal coupling, few-mode fiber

1. Introduction

In recent years, *fiber Bragg gratings* (FBGs) written in *large mode area* (LMA) and *few-mode* (FMF) optical fibers have become increasingly important due to their practical applications. Fiber Bragg gratings written in LMA fibers act as *high reflection* (HR) and low reflection (OC — *optical coupler*) mirrors in all-fiber high-power lasers [1]. Due to the larger core diameter of LMA fibers (and therefore the larger mode area with respect to the conventional *single-mode optical fibers* (SMF)), much more optical power can be guided without destructible nonlinear and material damage effects [2]. To provide single-mode or at most few-mode guidance in such fibers, it is necessary to decrease the *numerical aperture* (NA), i.e., to decrease core-cladding refractive index difference, which unfortunately results in a significant increase in bending losses. So, it is usually a trade-off between modality and bending sensitivity of LMA. This makes it necessary to consider the possibility of simultaneous excitation and propagation of the fundamental and higher modes in the spectral analysis of FBG written in LMA.

Few-mode fibers are intentionally designed to support multiple spatial modes. In the mode-division multiplexing technique, these modes act as individual communication channels, increasing data-carrying capacity [3]. Due to the different responses of fundamental and higher modes to external factors, such as bending, FMF with in-written FBG offers new opportunities for multi-parameter sensing. Moreover, FBGs written in FMF can induce mode coupling between propagating modes, leading to a more sensitive response to external perturbations [4]. FMF-based FBGs are also promising in advanced fiber lasers [5].

The development of new FBG-based devices and sensors in both LMA and FMF fibers requires reliable modeling and optimization. Commercially available software offers many possibilities in modeling fiber Bragg gratings, considering such aspects as the structure (refractive index profile) and modality of the fiber, photosensitivity profile, grating types and their dispersion properties. However, these software have their drawbacks, which limit the possibility of spectral analysis of FBG written in non-single-mode fibers. Although commercial software, such as OptiGrating, typically uses a mode solver to

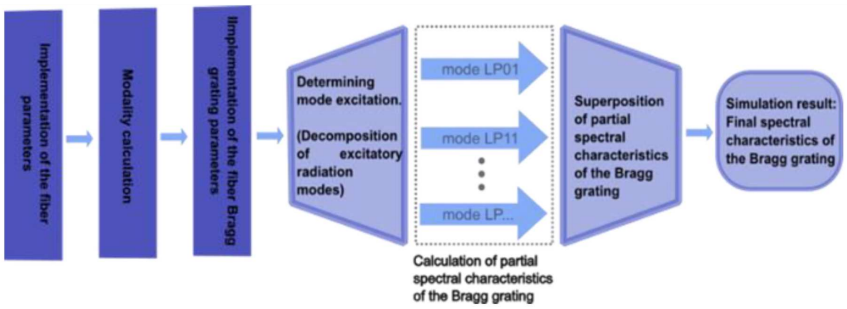

Fig. 1. The proposed algorithm of FBG spectral response calculation in LMA and FMF fibers under multi-mode excitation.

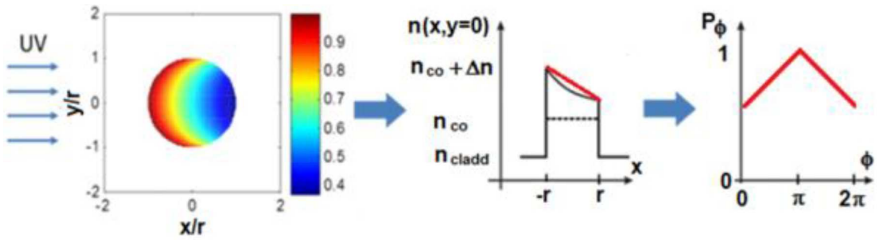

Fig. 2. Scheme of the FBG fringe pattern inhomogeneity implementation.

TABLE I

Parameters of nFMF fiber utilized in the simulations.

Parameter	Value
cladding diameter [μm]	140
cladding refractive index	1.44969
core diameter [μm]	17
core refractive index	1.45094
numerical aperture (NA)	0.06
V at 1060 nm	3.06

analyze the modality of optical fibers and takes into account the interaction of gratings with both core and cladding modes, it only allows the calculation of FBGs spectral responses when excited by a single, fundamental or higher mode. However, in practice, the few-mode (or more generally multi-mode) fibers exhibit multi-mode operation due to the simultaneous excitation of fundamental and higher modes.

In addition, for a reliable analysis of FBGs written in few-mode or multi-mode fibers, it is necessary to take into consideration the inhomogeneity in induced periodical fringe pattern during UV side-writing grating inscription. This non-uniformity causes intermodal coupling, which affects FBG spectral response [6].

To overcome the above limitations, a numerical tool has been developed that extends the capabilities of the commercial OptiGrating software. The idea of implementation of a complex excitation (with two or more modes simultaneously) scheme and its experimental validation are presented in Sect. 2. Subsequently, in Sect. 3, the spectral responses of FBGs written in *nanostructured large mode area* (nLMA) and *nanostructured few-mode fibers* (nFMF) are analyzed using this software. In particular, optimization of higher-order modes interaction with grating structures is examined by independent shaping of refractive index and photosensitivity profiles of optical fibers. Such an advanced tailoring of optical fiber properties fits the capabilities of recently developed free-forming (or nanostructuring) technology [7]. Section 4 summarizes the results of this work.

2. Numerical tool and its validation

2.1. Description of the simulation method

To calculate the spectral response of FBGs in optical fibers under few-mode excitation, the following algorithm was proposed. At first, the refractive index profile and photosensitivity profile were implemented in OptiGrating to calculate modes. Then, for established modes, the excitation scheme decomposition method was applied. It relies on the calculation of FBG responses when each fiber mode is separately excited. Then partial results, corresponding to every mode in the excitation scheme, are superposed, and thus, the final spectral response of FBG was obtained. The subsequent steps of the algorithm are shown in Fig. 1.

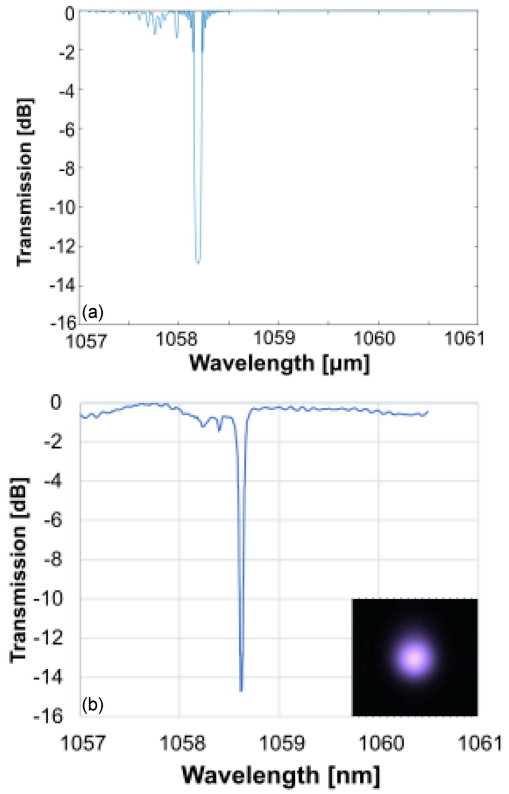

Fig. 3. Comparison of numerical (a) and experimental (b) results of the transmission spectrum of the FBG written in nLMA fiber under maximum excitation of the LP_{01} mode.

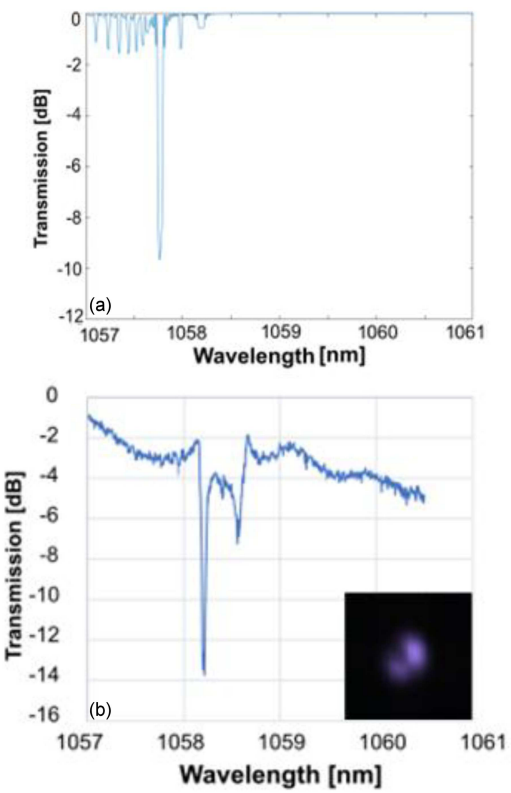

Fig. 4. Comparison of numerical (a) and experimental (b) results of the transmission spectrum of the FBG written in nLMA fiber under maximum excitation of the LP_{11} mode.

Additionally, to implement the inhomogeneity of induced periodic refractive index variations in the fiber core, the simple method was proposed according to the scheme shown in Fig. 2. When FBG is written using side-illumination with *ultraviolet* (UV) radiation, the amplitude of refractive index changes (Δn) approximately linearly decreases along the writing laser beam propagation direction due to the UV absorption. Thus, the linear decrease in Δn can be easily transformed into the triangular shape of the azimuthal photosensitivity profile P_ϕ.

2.2. Validation of the numerical tool

In order to validate the proposed numerical tool, simulation results were compared with experimental ones. For this purpose, FBGs were written in designed and fabricated nanostructured large mode area (nLMA) fiber [8]. The fiber was optimized to operate at 1060 nm for Yb-based laser application. The nLMA parameters used in FBG fabrication (and in simulation) are presented in Table I. The step-index profile of nLMA fiber and $V = 3.06$ ensures that at 1060 nm, two-mode operation (LP_{01} and LP_{11}) is supported.

Prior to the FBG inscription, nLMA fiber was hydrogen-loaded under high pressure (130 bars) for 3 weeks in order to increase its photosensitivity. Then FBGs with Bragg wavelength c.a. 1060 nm were written using a KrF excimer laser operating at 248 nm and a phase mask with a period of 729.6 nm. Spectral responses of in-written FBGs were measured using a broadband source (*superluminescent diode* — SLED) and *optical spectrum analyzer* (OSA) with 0.01 nm resolution. The selective mode excitation was achieved through the precise adjustment of light coupling from SMF to nLMA optical fiber. For this purpose, an ultra-precise XYZ translation stage and microscope objective were used. In addition, the mode filed distribution excited in nLMA fiber was observed by the CCD camera.

In the experiment, two cases were analyzed in which LP_{01} mode (Fig. 3) and LP_{11} mode (Fig. 4) were maximally excited. Finally, to compare collected spectra with numerical results, spectral responses of FBG in nLMA were calculated using proposed numerical tool for the following excitation conditions: (i) 95% of optical power in LP_{01} mode and 5% in LP_{11} mode (Fig. 3) and (ii) 12% of optical power in LP01 mode and 88% in LP_{11} mode (Fig. 5). Additionally, images of spatial

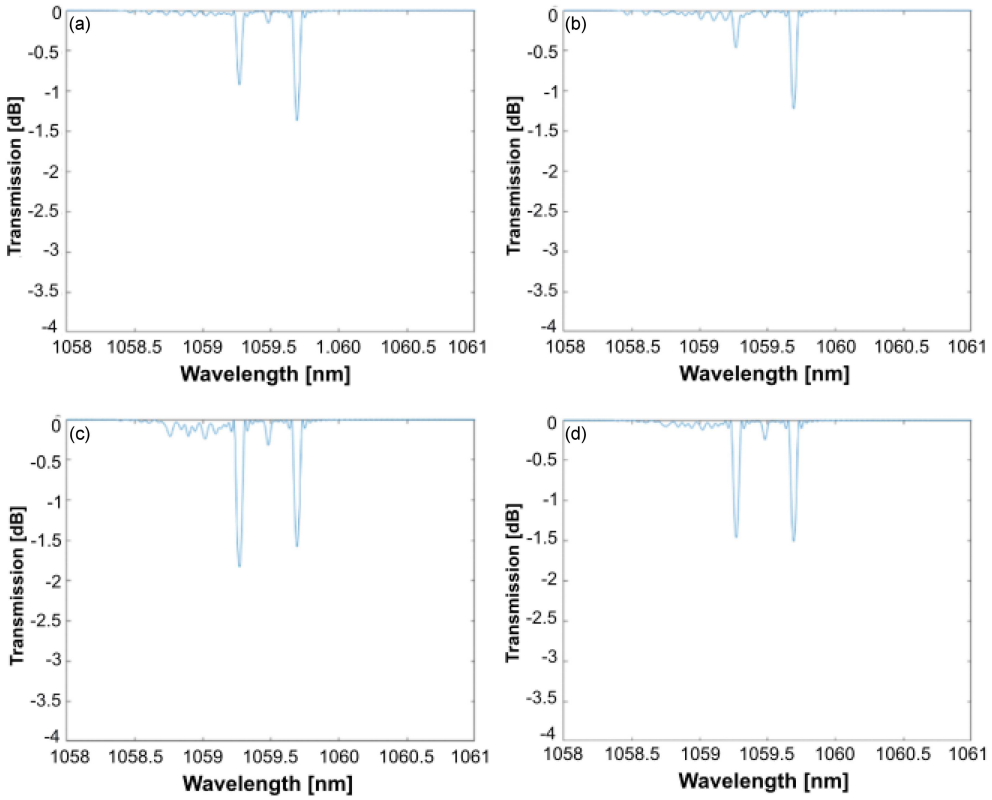

Fig. 5. Simulation results (a–d) of spectral responses of FBGs written in two-mode nLMA fiber with various radial photosensitivity profiles.

distribution of light in nLMA measured by CCD camera are presented as insets. Numerical calculations of FBG written in nLMA were carried out for grating parameters established through estimations based on experimental results ($\Delta n = 10^{-4}$) or adjusted to obtain similarity in transmission minima and the relationship between them (modal excitation scheme).

When the LP_{01} mode is maximally excited (Fig. 3), a high similarity between the computational and experimental results is achieved. The numerical results reveal a comb-like structure of the cladding modes, which corresponds to the similar envelope on the shorter-wavelength side of the Bragg wavelengths in the measured spectrum. This envelope is a consequence of the limited OSA resolution. Nevertheless, in both cases, Bragg minima, resulting from the interaction of the grating with the LP_{01} and LP_{11} modes, as well as the central minimum associated with the intermodal coupling, are clearly visible. When LP_{11} mode is maximally excited, a strong correlation between experimental and simulation results is also noticed. As before, the relationship between the Bragg minima corresponding to LP_{01} and LP_{11} modes and intermodal coupling is preserved. As in the previous case the comb-like cladding modes structure is visible in the measured spectrum in the form of a short-wavelength side envelope.

3. Numerical analysis of FBG written in nLMA fibers

Recently developed nanostructuration technology opens new possibilities in the design and fabrication of optical fiber [7]. Because in this technology, the optical fiber preform is composed of hundreds and even thousands of arbitrarily arranged nanorods of different types (including various dopants and their concentration), the refractive index and photosensitivity profiles can be designed independently. Based on this advantage of free-forming technology, the specially designed nLMA and nFMF were numerically analyzed in terms of the interaction efficiency of grating structure with high-order modes.

3.1. Step-index nLMA fibers with radially shaped photosensitivity profile

In order to optimize interactions between particular propagating modes with in-written grating, one can consider shaping the photosensitivity profile of the fiber core. In the OptiGrating environment, the photosensitivity profile $P(r, \phi)$ is defined as the product of the radial photosensitivity

profile P_r(r) and the azimuthal photosensitivity profile $P_\phi(\phi)$, according to the following relationship

$$P(r,\phi) = P_r(r)\, P_\phi(\phi), \tag{1}$$

where r and ϕ are the radial and azimuthal coordinates, respectively. Thus, by choosing an appropriate radial photosensitivity profile of the fiber core, it is possible to influence the efficiency of FBG reflection of light that propagates in a particular mode distribution. For this purpose, the same step-index refractive index profile of the nLMA fiber and various radial photosensitivity profiles were assumed, as shown in Fig. 6. The nLMA fiber parameters used in simulations are the same as in Table I. Moreover, two-mode operation (LP_{01} and LP_{11}) of nLMA and equal mode excitation were considered. The triangular azimuthal photosensitivity profile P_ϕ ensures that intermodal coupling is also considered. In Fig. 5, simulation results are presented. All spectral responses consist of two clearly visible Bragg minima that correspond to the LP_{11} (lower wavelength) and LP_{01} (higher wavelength) modes. There is also the third minimum between them that corresponds to the LP_{01}-LP_{11} mode coupling.

Simulation results reveal that the radial photosensitivity profile influences the reflection efficiency of particular modes by the grating. It can be noticed that the strong reflection of a particular mode is observed when the mode profile overlaps well with the photosensitivity profile of the fiber core. Extreme cases are presented in Fig. 5b and 5c. In Fig 5b, where the triangle profile fits well with the spatial (Gaussian) distribution of fundamental LP_{01} mode, the reflection of this mode is the most effective. On the other hand, Fig. 5c shows that for the donut-like photosensitivity profile the, LP_{11} mode is even more effectively reflected than the LP_{01} mode. This is due to the relatively better overlap of the donut-like photosensitivity profile with LP_{11} spatial mode distribution than with LP_{01} one.

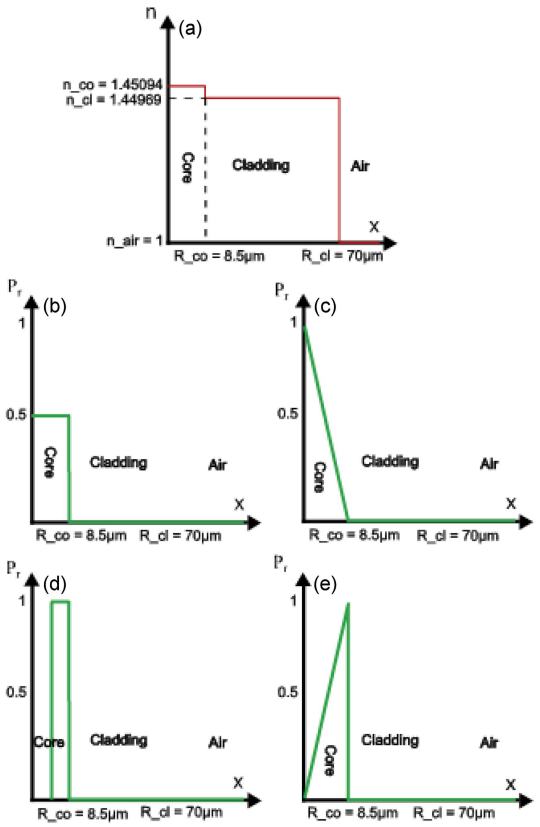

Fig. 6. Refractive index profile (a) and four radial photosensitivity profiles (b–e) of nLMA fiber used in the simulations.

TABLE II

Parameters of nFMF used in simulations.

Parameter	Value
cladding diameter [μm]	140
cladding refractive index	1.44969
core diameter [μm]	16
core refractive index	1.45192
numerical aperture (NA)	0.08
V at 1060 nm	3.81

3.2. nFMF fibers with radially shaped refractive index profiles

The optimization of the interaction of high-order modes with grating structure can also be achieved by modifying the mode profile while keeping the photosensitivity profile unchanged. Some of refractive index profiles may promote higher-order mode guidance while suppressing or not changing the fundamental mode. However, the previously researched fiber is unfit for this kind of modification as the refractive index difference is low and causes weak guiding of the LP_{11} mode (only around 67% of optical power in this mode is confined in the fiber core). To increase the power confinement factor of LP_{11} mode, the numerical aperture of the fiber was increased by enlarging the difference between the core and the cladding refractive indices. In this way, the proposed fiber can be assumed as nFMF. The parameters of nFMF used in simulations are presented in Table II.

These fiber parameters ensure that c.a. 83% of the optical power of LP_{11} mode is confined in the fiber core and two-mode operation is maintained. The equal mode excitation is assumed as well.

It is worth noting that FMFs usually have higher core diameters than SMF, which allows for the propagation of higher optical power in a few modes simultaneously without the occurrence of destructive nonlinear effects. Based on previously presented results, it was proven that the best interaction of grating structure with higher mode (LP_{11}) occurs for

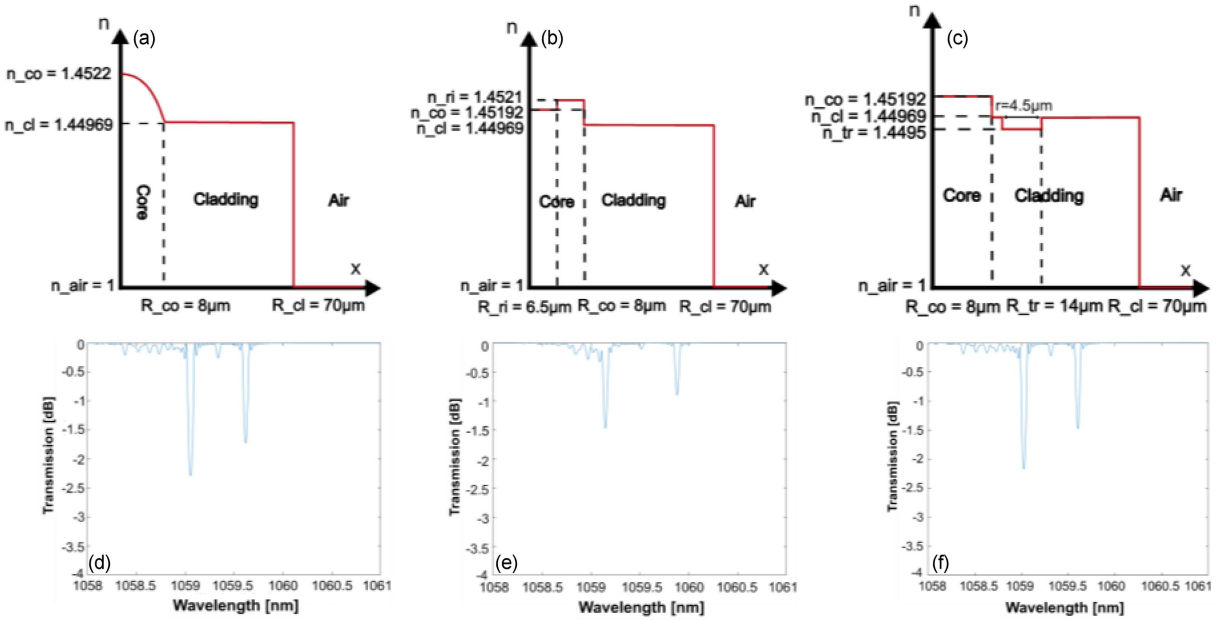

Fig. 7. The refractive index profiles (a–c) of nFMF and spectral responses of FBG in nFMF for these profiles (d–f).

the donut-like photosensitivity profile of the fiber core. Thus, this radial photosensitivity profile was used in these calculations, together with the previously mentioned triangular azimuthal photosensitivity profile, while three different refractive index profiles of nFMF were evaluated, as shown in Fig. 7. Specifically, graded-index and trench-assisted refractive index profiles were chosen because of their higher-order mode promoting characteristics [9].

Ring-core refractive index profile comes directly from the higher Ge concentration near the core-cladding interface, according to the assumed donut-like photosensitivity profile. The refractive index of the inner core can be increased by using non-photosensitive nanorods with a higher refractive index than pure silica. It is beneficial as the higher refractive index of the ring increases the LP_{11} mode confinement, enabling propagation with less attenuation. Graded-index profile promotes LP_{11} guidance with a different mechanism. Due to the parabolic profile's higher overall refractive index, the difference between the core and cladding can be applied while maintaining two-mode operation. This profile can be achieved by using the combination of nanorods (for example, F-doped) that decrease the refractive index in the area of higher Ge concentration and nanorods with a higher refractive index than pure silica in the inner core (un-doped area). The trench-assisted profile can be realized in a comparable way, however, additional refractive index reduced nanorods should be applied in the trench area of the fiber cladding. Simulation results are shown in Fig. 7. In each case, a stronger reflection of LP_{11} mode than of LP_{01} mode is observed. It is due to the donut-like radial photosensitivity profile. However, it is noticeable that the refractive index profile strongly influences both the reflection relation between Bragg minima associated with LP_{01} and LP_{11} modes and their spectral separation. This is because the refractive index profile influences the modal characteristics of nFMF fiber [10]. The intermodal coupling is also observed as a low minimum between the Bragg resonances.

4. Conclusions

The numerical tool for spectral analysis of FBGs written in few-mode excited optical fibers was proposed and successfully validated by comparison with experimental results. This tool, when supported by commercially available OptiGrating software, increases the versatility of spectral analysis of FBGs written in unconventional optical fibers, such as nLMA and nFMF. It was proven that due to the free-forming technology, the spectral behavior of Bragg gratings can be widely optimized by appropriate and independent tailoring of both modal and photosensitive properties of such few-mode optical fibers. It opens new possibilities in applications of FBGs written in specially designed FMF and LMA fibers in optical communication, fiber lasers, and sensing.

References

[1] H. Xiao, P. Zhou, X.L. Wang, S.F. Guo, X.J. Xu, *Laser Phys. Lett.* **9**, 748 (2012).

[2] R. Ahmad, M.F. Yan, J.W. Nicholson, K.S. Abedin, P.S. Westbrook. C. Headley, P.W. Wisk, E.M. Monberg, D.J. DiGiovanni, *Opt. Lett.* **42**, 2591 (2017).

[3] K. Kitayama, N.-P. Diamantopoulos, *IEEE Commun. Mag.* **55**, 163 (2017).

[4] I. Ashry, Y. Mao, A. Trichili, B. Wang, T.K. Ng, M.-S. Alouini, B.S. Ooi, *IEEE Access* **8**, 179592 (2020).

[5] W. Jin, Y. Qi, Y. Yang, Y. Jiang, Y. Wu, Y. Xu, S. Yao, S. Jian, *J. Opt.* **19**, 095702 (2017).

[6] Wu Chuang, Liu Zhengyong, Chung Kit Man, M.-L.V. Tse, F.Y.M. Chan, A.P.T. Lau, C. Lu, H.-Y. Tam, *IEEE Photon. J.* **4**, 1080 (2012).

[7] A. Anuszkiewicz, R. Kasztelanic, A. Filipkowski, G. Stepniewski, T. Stefaniuk, B. Siwicki, D. Pysz, M. Klimczak, R. Buczynski, *Sci. Rep.* **8**, 12329 (2018).

[8] A. Anuszkiewicz, M. Franczyk, D. Pysz, F. Wlodarczyk, A. Filipkowski, R. Buczynski, T. Osuch, *App. J. Light Technol.* **40**, 3947 (2022).

[9] L. Gruner-Nielsen, R.L. Lingle, D.W. Peckham, Y. Sun, "Multiple LP-mode Fiber Designs for Mode-division Multiplexing", European Pattent no. EP2706387A1, 2014.

[10] G.P. Agrawal, *Fiber-Optic Communication Systems*, John Wiley & Sons, Newark (NJ) 2010.